[9] P. Richardson, D. Flynn, A. Keane, "Optimal Charging of Electric Vehicles in Low-Voltage Distribution Systems", IEEE Transactions On Power Systems, Vol. 27, No. 1, February 2012.

[10] D. Nedeljković: "Električna mobilnost – z električnimi vozili ali s priključnimi hibridi?", Zbornik ERK 2012, Zv. A, str. 269–272, Portorož, Slovenija, 2012.

[11] S. G. Wirasingha, A. Emadi, "Pihef: Plug-In Hybrid Electric Factor", IEEE Transactions On Vehicular Technology, Vol. 60, No. 3, March 2011.

[12] S. G. Wirasingha, R. Gremban, A. Emadi, "Source-to-Wheel (STW) Analysis of Plug-in HybridElectric Vehicles" .IEEE Transactions On Smart Grid, Vol. 3, No. 1, March 2012.

[13] European Commission Regulation No 692/2008 [Online] http://eur-lex.europa.eu/LexUriServ/LexUriServ.do?uri=CELEX:32008R0692:en:NOT.

[14] U. S. Department of Energy, Environmental Protection Agency (EPA), The official U. S. goverment source for fuel economy information [Online]. http://www.fueleconomy.gov.

David Nedeljković je diplomiral leta 1991, magistriral leta 1996 in doktoriral leta 1998 na Fakulteti za elektrotehniko Univerze v Ljubljani. Zaposlen je kot profesor na Fakulteti za elektrotehniko Univerze v Ljubljani, kjer je od leta 2008 tudi prodekan za finančne zadeve. Ukvarja se s problematiko digitalnega procesiranja na področju naprav močnostne elektronike in elektromotorskih pogonov.

ELEKTROTEHNIŠKI VESTNIK 80(3): 79-83, 2013
ORIGINAL SCIENTIFIC PAPER

Dynamic Modeling, Control and Electromagnetic Transient Simulation of the Modular Cascaded Converters (MCCs)

Lin Xu

Sichuan Electric Power Research Institute, Sichuan Electric Power Corporation, STATE GRID. No.24, QingHua Road, QingYang District, 610072 Chengdu, China
E-mail: xulin198431@hotmail.com

Abstract. This paper presents the dc-link capacitor balancing control scheme and effective current regulation algorithms for the modular cascaded converters (MCCs). The analytical model for the dc-link voltage balancing and capacitor energy mechanism are presented. Based on the devised control models, an effective control method is devised for the dc-link capacitor voltages, i.e., the sum capacitor voltage controller (SCVC), difference capacitor voltage controller (DCVC). In order to improve the tracking accuracy of the current regulator, the model predictive current controller (MPCC) is devsied and implemented. To minimize the circulating current, an effective circulating current damping controller (CCDC) is proposed by using a proportional-resonant controller. Digital simulation of the single-phase five-level MCC is carried out using the Electromagnetic Transient Program, which confirms the validity of the devised algorithms.

Keywords: dynamic modeling, voltage control, electromagetic transients, proportional resonant controller.

1 INTRODUCTION

Large inverters have traditionally satisfied the ever-increasing demand of high-power applications, which currently extend from the tens to hundreds of megawatts. Some examples of this fact are the medium-voltage range (2.3 to 13.8 KV) AC motor drives. Nowadays, it is problematic to connect only one power semiconductor switch directly to the grid due to the high-voltage range. In order to solve this difficulty, a new type of the power converter has been introduced as a solution in high power applications [1-5].

Multilevel voltage-source converters (VSCs) allow a significant reduction of the harmonic content of the output voltage as compared to the traditional two-level VSCs [1]. Among the various multilevel topologies [2], the fairly recently proposed modular multilevel cascade converter (MMCC) [3] has many attractive properties. As the name suggests, the topology is modular and easily scalable in terms of voltage levels. It consists of *N* identical series-connected sub-modules per arm, which brings flexibility to the circuit design, and results in low-voltage steps [4, 5].

Multilevel converters use high-speed switching components, avoiding the problem of linking them directly to the grid by connecting single devices among multiple DC levels. Multilevel converters are found in many applications, such as industrial motor drives, utility interfaces for the renewable energy systems (photovoltaic, wind energy and fuel cells), flexible AC transmission systems (FACTS), high-voltage direct current transmission (HVDC), and traction drives systems [3].

Figure 1 shows the circuit diagram of the three-phase modular cascaded converter (MCC) topology, consisting of six leg-arms, with *n* identical half-bridge converter submodule in each leg-arm. Each module is consists of two IGBTs and two anti-parallel diodes, and

Received 25 April 2013
Accepted 29 July 2013

with a dc-link capacitor. When the upper IGBT is on and the lower IGBT is off, the module is switched on. Conversely, when the lower IGBT is on and the upper IGBT is off, the submodule is switched off. By dynamically controlling the switching states of the IGBTs in each converter arm, the output multilevel voltage can be synthesized, thus the high-power MCC can be realized.

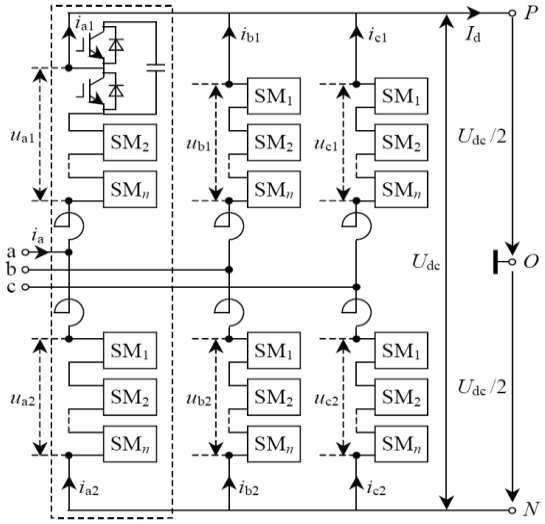

Figure 1. Circuit diagram of the three-phase MCC topology.

In high-voltage applications, n may be as high as several hundreds, which is an ideal choice for high-voltage high-power applications, such as HVDC, high-power motor drives, and electric railway supplies [5-8]. The grid-connected MCC may act as a rectifier, inverter, inductor, and capacitor, depending on the phase difference between the supply voltage and current. This implies that the MCC is required to achieve rigid and stable voltage control of all the floating dc capacitors under all operating states.

This paper presents the dc-link capacitor balancing and effective current control methodologies for the MCC. Organization of this paper is as follows. Section 2 presents the system description of the MCC system. Section 3 presents the modeling and analysis of the MCC. Section 4 presents the control strategies of the MCC, including the sum capacitor voltage controller (SCVC), the difference capacitor voltage controller (DCVC), the predictive current loop controller (PCC) and the circulating current damping controller (CCDC). Section 5 presents the simulation results. Section 6 concludes the paper.

2 Introduction of the Modular Cascaded Converter (MCC)

Figure 2 shows the circuit diagram of the single-phase MCC. The dc side of the MCC is denoted by two series-connected DC voltage sources $V_d/2$. The buffer inductance and resistance are denoted as L_e and R_e, respectively. The upper arm and lower arm contain two half-bridge chopper cells with equal dc-link capacitors. The output of the MCC is connected to the grid through the coupling inductance L, which is omitted in Figure 2 for the sake of brevity. Figure 3 shows the detailed illustration of the submodule and the available power-electronic devices HVIGBT, IGBT Presspack and the IGCT Presspack [1, 2].

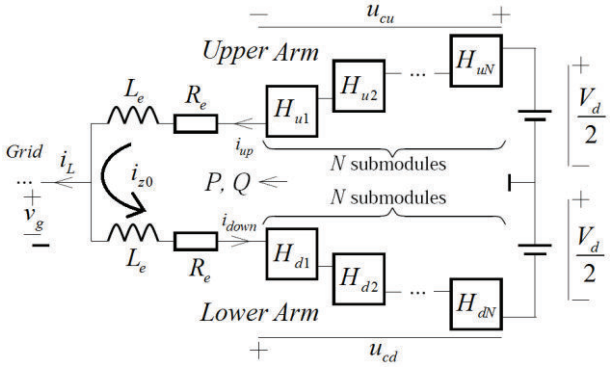

Figure 2. Circuit diagram of the single-phase MCC topology.

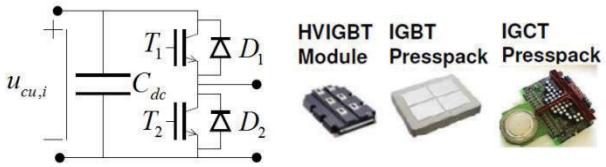

Figure 3. The detailed illustration of the submodule and the available power electronic devices HVIGBT, IGBT Presspack and the IGCT Presspack.

3 Dynamic Modeling of the Modular Cascaded Converter (MCC)

To derive the mathematical model of the MCC converter, let us consider a generic converter with N sub-modules per arm, each arm is controlled with the modulation index $m(t)$, where $m(t)$=0 and $m(t)$=1mean that all sub-modules in the arm are either by-passed or inserted. The ideal capacitance of the arm is denoted as:

$$C_{u,d} = C_{dc} / N \tag{1}$$

where $C_{u,d}$ denotes the capacitance of each chopper cell. Therefore, the following equation holds for the upper leg currents:

$$\frac{d\sum u_{dc,u}(t)}{dt} = \frac{m_u(t) i_u(t)}{C_u} \tag{2}$$

The similar equation can be bulit for the lower leg.

Referring to Fig.1, when only the single-phase leg is considered, and introducing the current i_{z0}

$$i_{z0} = \frac{i_u + i_d}{2}, \quad i_u = \frac{i_L}{2} + i_{z0}, \quad i_d = -\frac{i_L}{2} + i_{z0} \tag{3}$$

where i_u and i_d represent the upper and lower arm currents. Hence, the load current is represented as:

$$i_L = i_u - i_d \tag{4}$$

From Fig.2, the following equations are derived by using the Kirchhoff's Voltage Law (KVL):

$$\left.\begin{aligned}\frac{V_d}{2}-R_e i_u-L_e\frac{di_u}{dt}-m_u\sum u_{dc,u}\\ -\frac{V_d}{2}+R_e i_d+L_e\frac{di_d}{dt}+m_d\sum u_{dc,d}\end{aligned}\right\}=u_v \tag{5}$$

where u_v denotes the voltage at the center of the converter leg.

According to Eq.(5), we can get:

$$u_{z0}=R_e i_{z0}+L_e\frac{di_{z0}}{dt}=\frac{V_d}{2}-\frac{m_u\sum u_{dc,u}+m_d\sum u_{dc,d}}{2} \tag{6}$$

$$u_v=\frac{m_u\sum u_{dc,u}-m_d\sum u_{dc,d}}{2}-\frac{R_e}{2}i_L-\frac{L_e}{2}\frac{di_L}{dt} \tag{7}$$

where u_{z0} denotes the voltage drop across the R_e and L_e. From Eq.(6) and Eq.(7), we get:

$$\frac{d\sum u_{dc}(t)}{dt}=\frac{N}{C_{dc}}(m_u i_u+m_d i_d) \tag{8}$$

$$\frac{d\Delta u_{dc}(t)}{dt}=\frac{N}{C_{dc}}(m_u i_u-m_d i_d) \tag{9}$$

where $\sum u_{dc}(t)$ and $\Delta u_{dc}(t)$ denote the sum and difference between $\sum u_{dc,u}(t)$ and $\sum u_{dc,d}(t)$. The modulation index m_u and m_d can be denoted as:

$$m_u=\frac{1}{2}-\frac{u_v+u_{z0}}{V_d},\ m_d=\frac{1}{2}+\frac{u_v-u_{z0}}{V_d} \tag{10}$$

From Eqs.(6)-(10), we get:

$$\frac{d\sum u_{dc}(t)}{dt}=\frac{N}{C_{dc}}[-\frac{u_v i_L}{V_d}+(1-\frac{2u_{z0}}{V_d})i_{z0}] \tag{11}$$

$$\frac{d\Delta u_{dc}(t)}{dt}=\frac{N}{C_{dc}}[(\frac{1}{2}-\frac{u_{z0}}{V_d})i_L-\frac{2u_v i_{z0}}{V_d}] \tag{12}$$

From Eq.(6), the MMCC system dynamic charercter can be described as:

$$\begin{aligned}\frac{di_{z0}}{dt}=&\frac{V_d}{2L_e}-(\frac{1}{4L_e}-\frac{u_{z0}}{2V_d L_e})\sum u_{dc}(t)\\ &-\frac{u_v}{V_d L_e}\Delta u_{dc}(t)-\frac{R_e}{L_e}i_{z0}\end{aligned} \tag{13}$$

The approximated steady state solution of i_{z0} can be derived from Eq.(13) by assuming the u_{z0} is smaller compared with V_d, thus we get:

$$i_{z0}=\frac{u_v i_L}{V_d} \tag{14}$$

Therefore, the u_{z0} is derived as:

$$u_{z0}=\frac{V_d}{2}-\frac{2u_v^2}{V_d} \tag{15}$$

Assuming the output voltage u_v is as followed :

$$u_v=V_m\sin(\omega t) \tag{16}$$

Either in the active power or in the reactive power transmission mode , i_{z0} can be derived as:

$$i_{z0}=\begin{cases}\dfrac{V_m I_{Lm}}{2V_d}(1-\cos(2\omega t))\\ \dfrac{V_m I_{Lm}}{2V_d}\sin(2\omega t)\end{cases} \tag{17}$$

when I_{Lm} represents the amplitude of i_L. i_{z0} contains a second order oscillation term, which causes unnecessary circulating currents and power loss across the arms. Similarly, when the converters work in the harmonic compensation mode, the even harmonic oscillation is appeared. Therefore, it is necessary to minimize the power loss generated by i_{z0}.

4 CONTROL STRATEGIES OF THE MCC

Figure 4 shows the control architecture for the proposed MCC,which is implented in EMTP simulation platform. The devised control strategies of the MCC include the sum capacitor voltage controller (SCVC) , the difference capacitor voltage controller (DCVC) and the current tracking controller (CC). The SCVC block is used to control the whole energy of the leg, and the DCVC block is used to keep the balance between upper and lower arms of the MMCC phase-leg. Since total energy and energy balance interacts dynamically, the DCVC loop is tuned to be about ten percent of the SCVC loop in order to achieve the decoupled control.

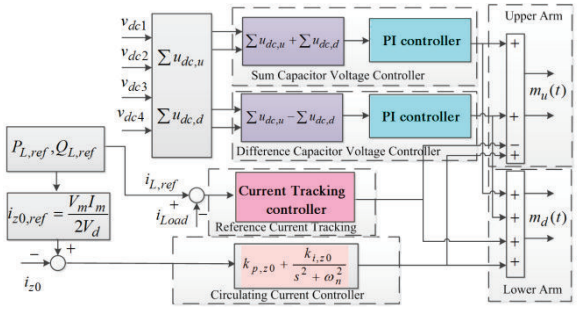

Figure 4.The control block diagram of the MCC system.

4.1 Sum-Capacitor Voltage Controller

It is well known that the active and reacitve power transmission between the converter and the grid depends on the magnitude and phase of the synthesized multilevel voltage u_{cu} (u_{cd}) with respect to the grid voltage v_g. To control the total energy stored in the MCC converter leg, the sum-capacitor voltage controller (SCVC) is used. One input of the controller is sum of all the dc-link capacitor voltage, and another is the reference voltage which is set to $2V_d$. It was found that the proportional-integral (PI) controller is sufficient to control the error between sum-capacitor voltage and its reference, which is crucial to ensure global stability under a wide operation range .

4.2 Difference-Capacitor Voltage Controller

In addition to the sum-capacitor voltage controller, which regulates the total active power absorption of MCC, the difference capacitor voltage should also be

regulated. Referring to Eq (12), the term i_L is not producing any average value since it is an AC component in steady state. The term $-2i_{z0}u_v/V_d$ also contributes only by an oscillating term, if i_{z0} does not have any component with the same frequency as u_v. The only quantity that can be freely varied without causing deviations from u_v reference is i_{z0}. Therefore, the only way to essume the energy balance between the two arms is to control the circulating current i_{z0}. Similarly, the PI controller is utilized to control the difference capacitor voltage to its reference (zero).

4.3 *Current Tracking Controller*

From Figure 2. The differential equation across the grid impedance is described as:

$$v_g = u_v + r_L \cdot i_L + L \cdot \frac{di_L}{dt} \tag{18}$$

where L and r_L denote the grid coupling inductance and its equivalent resistance. Applying Laplace transform to Eq.(18), and assuming $v_{dis} = v_g - u_v$, the following equation can be derived:

$$\frac{I_L(s)}{V_{dis}(s)} = \frac{1}{r_L + L \cdot s} \tag{19}$$

The open-loop transfer function for the current tracking controller G_{open} can be represented as:

$$G_{open}(s) = G_{cc}(s) \cdot \frac{1}{1 + T_d \cdot s} \cdot \frac{1}{r_L + L \cdot s} \tag{20}$$

where T_d denotes the control delay time, $G_{cc}(s)$ represents the transfer function of the current controller, which can be a proportional-integral (PI) controller or the proportional resonant (PR) controller. However, the PI regulator shows unsatisfatory performance for current tracking of alternating reference signal, which results in remarkable phase and amplitude errors. On the other hand, the PR controller can achieve perfect tracking performance for the alternating signal, which mimics the PI regulator implemented in the synchronous reference frame with the following transfer function:

$$G_{cc}(s) = K_P + \sum_{n=1}^{N} \frac{nK_{rn}\omega_0 s}{s^2 + n\omega_0 s/Q + (n\omega_0)^2} \tag{21}$$

where K_P is the proportional gain, K_{rn} is the gain of resonant term at nth order harmonic, ω_0 is the fundamental angular frequency of the grid voltage, and Q is the quality factor.

Notably, a higher Q results in higher resonant peak in the frequency domain characteristics, narrower bandwidth and increased oscillation in current tracking. On the other hand, if Q is selected too small, the steady-state error would be increased. Therefore, in order to achieve zero steady-state error and sufficient robustness, a tradeoff must be made when selecting the parameter Q. The value Q, K_P, K_{rn} and additional poles and zeros must be carefully evaluated, particularly with consideration to system stability and robustness. Usually, the genetic algorithm is used for parameter selection and optimization.

Similarly, the circulating-current damping controller (CCDC) is utilized by PR controller, where n=2, It is realized to eliminate the oscilation of the alternating signal at 100Hz .

5 SIMULATION RESULTS

To validate the effectiveness of the control strategies, the digital simulation of the single-phase five-level MCC is carried out using the Electromagnetic Transient Program (EMTP-ATP). The Transient Analysis of Control System (TACS) and the MODEL language in the EMTP are utilized to implement the control algorithms.

The system parameters are: the buffer inductance and resistance L_e=4.5mH, R_e=0.03Ohm, V_d=4500V, the dc-link capacitor value C_{dc}=2.5mF, the grid inductance L_s=5.5mH, V_{grid}=2kV (RMS), the capacitor reference dc-link voltage $V_{dc,ref}$=2250V.

Figure 6 and Figure 7 show the simulation results of the MCC under active power transmission mode without and with circulating current damping controller, respectively. The reference power is set as P_{ref}=0.2MW. The grid voltage undergoes abrupt sag of 0.3pu during 0.1s~0.2s. The dc-link capacitor voltages u_{dc1}~u_{dc4}, the load current i_L, the load voltage v_{Load}, the grid voltage v_{grid}, and the circulating current i_{z0} can be observed. In Figure 6, the peak active current reference $i_{L,ref}$=200A, it can be observed that the dc-link capacitor voltages of each leg are stable both in steady state and transient process, and i_{z0} shows obvious second order oscillation with positive dc offset without the circulating current controller. Meanwhile, it can be observed from Figure 7 that when the circulating current damping controller is activated, the second order oscillation is eliminated.

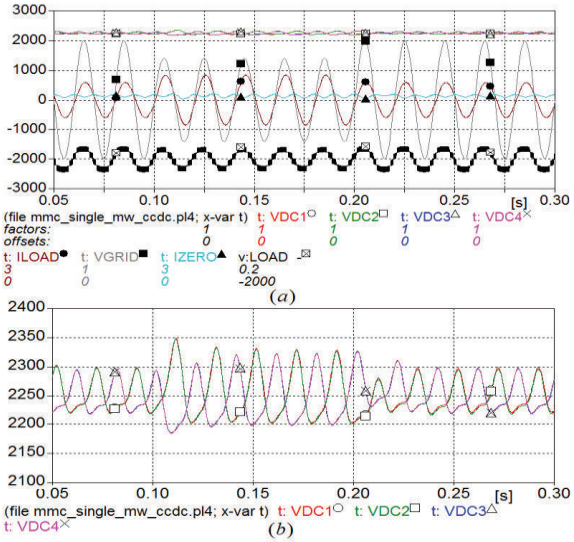

Figure 6. The simulation results of MCC for active power transmission without circulating current damping controller. (a). The dc-link voltages, ac-side current, the grid voltage and output multilevel voltage; (b). The enlarged view of the dc-link capacitor voltages.

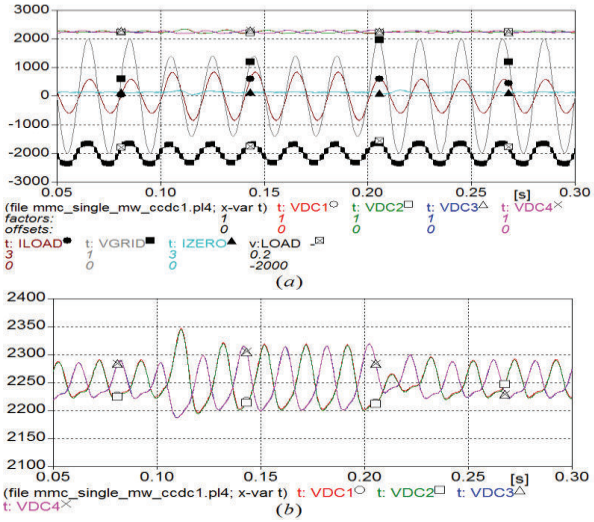

Figure.7. The simulation results of MCC for active power transmission with circulating current damping controller.

Similarly, Figure 8 and Figure 9 show the simulation results of the MCC under reactive power transmission mode without and with circulating current damping controller, respectively.And the reference power is Q_{ref}=0.2MWVar. The grid voltage undergoes abrupt sag of 0.3pu during 0.1s~0.2s. It can be observed from Fig.9 second order oscillation is eliminated when the circulating current damping controller is activated, and the circulating current is almost zero since the active power transmission of the MCC system is zero.

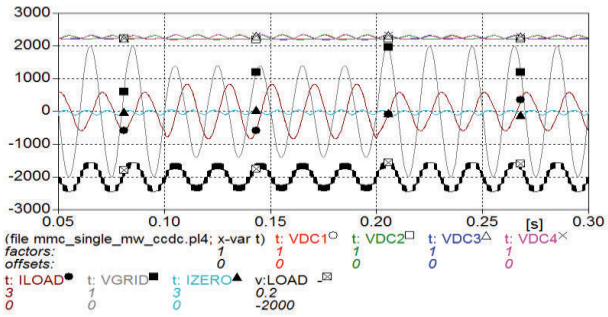

Figure 8. The simulation results of MCC for reactive power transmission without circulating current damping controller.

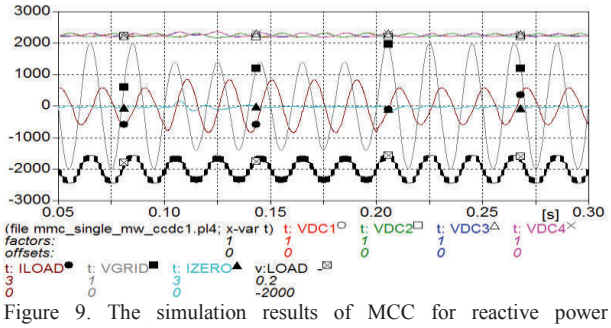

Figure 9. The simulation results of MCC for reactive power transmission with circulating current damping controller.

6 Conclusion

The paper proposes dc capacitor balancing and effective-current control methodologies for the modular multilevel cascaded converter (MCC). Based on the capacitor energy-evolving mechanism, an effective capacitor-control scheme is devised, which includes the sum-capacitor voltage controller (SCVC) and the difference-capacitor voltage controller (DCVC). To enhance the tracking accuracy of the current-control loop, a predictive current controller (PCC) is presented. To minimize the circulating current of the MCC, an effective circulating-current damping controller (CCDC) is proposed using a proportional-resonant controller. The simulation results under the active rectifier and the reactive compensation modes are presented for verification, which shows perfect capacitor-voltage balancing control and precise current tracking.

REFERENCES

[1] M. Hagiwara and H. Akagi, “Control and experiment of pulse-width modulated modular multilevel converters,” IEEE Trans. Power Electron., vol. 24, no. 7, pp. 1737–1746, Jul. 2009.

[2] M. Hagiwara, K. Nishimura, and H. Akagi, “A medium-voltage motor drive with a modular multilevel PWM inverter,” IEEE Trans. Power Electron., vol. 25, no. 7, pp. 1786–1799, Jul. 2010.

[3] H. Akagi, “Classification, Terminology, and Application of the Modular Multilevel Cascade Converter (MMCC),” IEEE Trans. Power Electron., vol. 26, no. 11, pp. 3119–3130, Nov. 2011.

[4] H. Peng, M. Hagiwara, H. Akagi, Modeling and Analysis of Switching-Ripple Voltage on the DC Link Between a Diode Rectifier and a Modular Multilevel Cascade Inverter (MMCI), IEEE Trans. Power Electron., vol. 28, no. 1, pp. 75–84, Jan. 2013.

[5] C. Gao, X. Jiang, Y. Li, Z. Chen, J. Liu, A dc-link voltage self-balance method for a diode-clamped modular multilevel converter with minimum number of voltage sensors, IEEE Transactions on Power Electronics, 28(5), 2125-2139, March 2013

[6] J. Gholinezhad, Analysis of cascaded Analysis of Cascaded H-Bridge Multilevel Inverter in DTC-SVM Induction Motor Drive for FCEV, Journal of Electrical Engineering and Technology, vol.8, no.2, pp.304-315, March 2013.

[7] M.R. Banaei, Asymmetric Cascaded Multi-level Inverter: A Solution to Obtain High Number of Voltage Levels, Journal of Electrical Engineering and Technology, vol.8, no.2, pp.316-325, March 2013.

[8] M.R. Banaei, Reduction of Components in Cascaded Transformer Multilevel Inverter Using Two DC Sources, Journal of Electrical Engineering and Technology, vol.7, no.4, pp.538-545, Jul. 2012.

Lin Xu received her B. E. degree in electrical engineering from University of Electronic Science and Technology of China (UESTC), Chengdu, China, in 2006, and her Ph.D. degree in electrical engineering from Shanghai JiaoTong University (SJTU), Shanghai, China, in 2011. Currently, she is working at Sichuan Electric Power Research Institute, Chengdu, China. Her research interests include power-system analysis and real-time digital simulator (RTDS), flexible ac transmission systems (FACTS), such as TCSCs, STATCOMs, and power-quality conditioners (DVRs, APFs). She is an active reviewer for the IEEE Transactions on Industrial Electronics, IEEE Transactions on Power Electronics, Electric Power Components and Systems.